
Research Article: Methods/New Tools | Novel Tools and Methods

An ATF3-CreERT2 knock-in mouse for axotomy-induced genetic editing: proof of principle.

Seth D Holland¹, Leanne M Ramer², Stephen B McMahon³, Franziska Denk³ and Matt S Ramer¹

¹*International Collaboration on Repair Discoveries, the University of British Columbia, Vancouver, BC, Canada*

²*Biomedical Physiology and Kinesiology, Simon Fraser University, Burnaby, BC, Canada*

³*Wolfson Centre for Age-Related Diseases, King's College London, London, UK*

<https://doi.org/10.1523/ENEURO.0025-19.2019>

Received: 19 January 2019

Revised: 18 March 2019

Accepted: 20 March 2019

Published: 28 March 2019

S.D.H., S.B.M., F.D., and M.S.R. designed research; S.D.H., L.M.R., and M.S.R. performed research; S.D.H. and M.S.R. analyzed data; S.D.H., L.M.R., F.D., and M.S.R. wrote the paper.

Funding: International Foundation for Research in Paraplegia (IRP)

;

Funding: Wellcome Trust (Wellcome)

.

Conflict of Interest: Authors report no conflict of interest.

The International Foundation for Research in Paraplegia (MSR), the Wellcome Trust (FD).

Correspondence should be addressed to Matt S Ramer at ramer@icord.org

Cite as: eNeuro 2019; 10.1523/ENEURO.0025-19.2019

Alerts: Sign up at www.eneuro.org/alerts to receive customized email alerts when the fully formatted version of this article is published.

Accepted manuscripts are peer-reviewed but have not been through the copyediting, formatting, or proofreading process.

Copyright © 2019 Holland et al.

This is an open-access article distributed under the terms of the Creative Commons Attribution 4.0 International license, which permits unrestricted use, distribution and reproduction in any medium provided that the original work is properly attributed.

1 Manuscript Title: **An ATF3-CreERT2 knock-in mouse for axotomy-induced genetic editing:**
2 **proof of principle.**

3
4 Abbreviated Title: **Axotomy-induced genetic editing**

5
6 Seth D Holland¹, Leanne M Ramer², Stephen B McMahon³, Franziska Denk³, and Matt S
7 Ramer^{1*}

8
9 ¹International Collaboration on Repair Discoveries, the University of British Columbia,
10 Vancouver, BC, Canada

11 ²Biomedical Physiology and Kinesiology, Simon Fraser University, Burnaby, BC, Canada

12 ³Wolfson Centre for Age-Related Diseases, King's College London, London, UK

13
14 SDH, FD, SBM and MSR designed research; SDH, LMR and MSR performed research, SDH
15 and MSR analyzed data; SDH, LMR, FD and MSR wrote the paper.

16
17 * Correspondence should be addressed to

18 Matt S Ramer

19 ICORD, 818 10th Ave. W.,

20 Vancouver, BC, Canada

21 V5Z1M9

22 ramer@icord.org

23
24 Number of Figures: 7

25 Number of words for Abstract: 250

26 Number of words for Significance Statement: 119

27 Number of words for Introduction: 749

28 Number of words for Discussion: 1655

29

30 Acknowledgements

31

32 Authors report no conflict of interest.

33

34 Funding sources: The International Foundation for Research in Paraplegia (MSR), the Wellcome
35 Trust (FD).

36

An ATF3^{cre} mouse for axotomy-induced genetic editing.

37 **An ATF3-CreERT2 knock-in mouse for axotomy-induced genetic editing: proof of**
38 **principle.**
39

40 **ABSTRACT**

41 Genome editing techniques have facilitated significant advances in our understanding of
42 fundamental biological processes, and the Cre-Lox system has been instrumental in these
43 achievements. Driving Cre expression specifically in injured neurons has not been previously
44 possible: we sought to address this limitation in mice using a Cre-ERT2 construct driven by a
45 reliable indicator of axotomy, Activating Transcription Factor 3 (ATF3). When crossed with
46 reporter mice, a significant amount of recombination was achieved (without tamoxifen
47 treatment) in peripherally-projecting sensory, sympathetic, and motoneurons after peripheral
48 nerve crush in hemizygotes (65-80% by 16 days) and was absent in uninjured neurons.
49 Importantly, injury-induced recombination did not occur in Schwann cells distal to the injury,
50 and with a knockout-validated antibody we verified an absence of ATF3 expression. Functional
51 recovery following sciatic nerve crush in ATF3-deficient mice (both hemi- and homozygotes)
52 was delayed, indicating previously unreported haploinsufficiency. In a proof-of-principle
53 experiment, we crossed the ATF3-CreERT2 line with a floxed PTEN line and show significantly
54 improved axonal regeneration, as well as more complete recovery of neuromuscular function.
55 We also demonstrate the utility of the ATF3-CreERT2 hemizygous line by characterizing
56 recombination after lateral spinal hemisection (C8/T1), which identified specific populations of
57 ascending spinal cord neurons (including putative spinothalamic and spinocerebellar) and
58 descending supraspinal neurons (rubrospinal, vestibulospinal, reticulospinal and hypothalamic).
59 We anticipate these mice will be valuable in distinguishing axotomized from uninjured neurons

An ATF3^{cre} mouse for axotomy-induced genetic editing.

60 of several different classes (e.g. *via* reporter expression), and in probing the function of any
61 number of genes as they relate to neuronal injury and regeneration.

62 **SIGNIFICANCE STATEMENT**

63 Understanding reactions to neurotrauma and overcoming obstacles to neural regeneration should
64 benefit from the ability to genetically label or otherwise edit the genome of injured neurons. We
65 sought to achieve this in mice by driving Cre recombinase expression under the control of
66 Activating Transcription Factor (ATF3), which is robustly induced by axotomy in several
67 populations of peripheral and central neurons. When crossed with reporter mice, recombination
68 occurred only in injured neurons following sciatic nerve injury or spinal hemisection. Peripheral
69 nerve injury-induced neuronal PTEN excision also resulted in improved regeneration and more
70 complete functional recovery. These results demonstrate the feasibility and utility of axotomy-
71 induced recombination and represent a new tool for investigating genetic control of injury
72 responses and regeneration.

73

74 **INTRODUCTION**

75 Advances in genome editing techniques have created opportunities to dissect out the
76 function of specific genes and their contributions to health and disease. Among the most widely
77 used of these tools is the Cre-Lox system, in which Cre expression can be restricted spatially, to
78 a single tissue or population of cells through insertion under a specific promoter (Wagner et al
79 1997, Clausen et al 1999, Agarwal et al 2004), or temporally, by fusing the protein to a mutated
80 estrogen receptor selective for tamoxifen (Indra et al 1999, Hayashi & McMahon 2002, Leone et
81 al 2003). In neurotrauma, the combination of spatial and temporal control of gene expression has
82 facilitated the identification of the function of individual neural cells (Sainsbury et al 2002,

An ATF3^{cre} mouse for axotomy-induced genetic editing.

83 Mishida et al 2003, Liu et al 2010), and manipulated their phenotype to promote repair of the
84 damaged nervous system (Park et al 2008, Sun et al 2011). A limitation in applying Cre-Lox to
85 investigations of neurotrauma is the inability to selectively express Cre in populations of neurons
86 affected by unique pathologies, such as tau protein-associated degeneration, immune-mediated
87 degradation, or simple axotomy. This could notionally be achieved by taking advantage of a gene
88 that is highly expressed only when the neuron is degenerating or axotomized. Pathology-induced
89 recombination would be of use to both identify the affected cell populations and to edit those
90 populations' genetic makeup. Here we present a novel transgenic approach to effecting genome
91 editing upon axotomy *via* an injury-specific gene.

92 Activating Transcription Factor 3 (ATF3) is a transcription factor that belongs to the basic
93 leucine zipper family (Liang et al 1996). ATF3 is an immediate early gene; its transcription is
94 initiated extremely rapidly following the appropriate stimulus. ATF3 is considered a reliable
95 marker of neuronal somata with injured peripheral axons (Tsujino et al 2000, Mason et al 2003);
96 ATF3 mRNA can be detected after peripheral axotomy as early as 6 hours after injury (Tsujino
97 et al 2000) and can achieve a 130-fold increase 72 hours post axotomy (Seijffers et al 2007).
98 Other genes upregulated following injury include c-Jun and GAP-43 (Tetzlaff et al 1991, Broude
99 et al 1997), but none are upregulated as fast and prominently as ATF3, making it the most
100 reliable marker of peripheral nervous system (PNS) injury. These changes in gene expression
101 constitute part of the pro-regenerative “cell body response” to injury. A loss of ATF3 function
102 has been shown to reduce the regeneration observed after a peripheral nerve injury (PNI) (Gey et
103 al 2016).

104 Damage to the PNS is a common outcome of motor vehicle accidents, penetrating trauma,
105 and falls (Kouyoumdjian, 2006). The PNS has the ability to regenerate injured axons that result

An ATF3^{cre} mouse for axotomy-induced genetic editing.

106 in full functional recovery: however, despite the theoretical regenerative capacity of the PNS,
107 clinical peripheral nerve injury (PNI) often results in permanent disability, since regeneration is
108 often incomplete when the distance from the axotomy to the soma is far, the gap between distal
109 and proximal stumps is large, or the time until surgical intervention is long. Reports suggest that
110 ~5% of all patients admitted to a level 1 trauma center sustained a PNI (Noble et al 1998),
111 highlighting the need for strategies that augment this inadequate regenerative response.

112 Phosphatase and Tensin Homologue (PTEN) is an inhibitor of the PI3K/AKT/mTOR cell
113 growth and proliferation pathway (Stambolic et al 1998). The loss of PTEN function *via* viral
114 Cre transfection induces a regenerative response in corticospinal neurons after a spinal cord
115 injury (Liu et al 2010), a finding that has been reported in other central nervous system (CNS)
116 axonal injury models (Park et al 2008). In the PNS, in which regeneration is more robust but still
117 suboptimal, PTEN deletion has been shown to have modest augmentative effects on axonal
118 regeneration (Gallaher & Steward, 2018). This allows for the unique opportunity to compare a
119 pathology-dependent Cre upregulation strategy with a more traditional viral Cre transfection
120 model.

121 Here we present a novel transgenic mouse model that allows for the selective genetic
122 editing of injured neurons via the insertion of a Cre-ERT2 construct under the native ATF3
123 promoter. We confirm expression of the Cre-ERT2 construct in injured neurons after PNI using a
124 fluorescent reporter line and we demonstrate that this model may also be used to effect
125 recombination in select populations of axotomized CNS neurons. Finally, we show that neuronal
126 injury-specific Cre-ERT2 expression can be used to functionally alter the regenerative capacity
127 of neurons though excision of crucial PTEN exons, a proof-of-principle experiment that
128 illustrates the utility and potential of this model in neurotrauma.

An ATF3^{cre} mouse for axotomy-induced genetic editing.

131 **MATERIALS & METHODS**

132 **Animals**

133 All animal procedures were performed in accordance with the University of British
134 Columbia and King's College London animal care committees' regulations. All mice were
135 between 2 and 4 months of age and equally distributed between sexes.

136 The ATF3-CreERT2 (ATF3^{cre}) strain used was generated and described by Denk et al.
137 (2015). Briefly the Cre-ERT2 construct was inserted directly after the ATG start codon of the
138 second ATF3 exon followed by a 3' untranslated region and a polyadenylation tagging sequence.
139 For some experiments this line was subsequently crossed to a floxed stop tdTomato Ai14
140 reporter line (JAX 007908) (Madisen et al 2010). The ATF3^{cre} line was also crossed with
141 conditional PTEN deletion line (PTEN^{fl/fl}) with LoxP sites flanking exon 5 of the PTEN gene
142 (JAX 006440) (Lesche et al., 2002) (in some cases also crossed with the Ai14 line to determine
143 recombination efficiency). Mice were maintained on a mixed C57BL/6J x 129SvEv background.
144 ATF3-CreERT2 mice are available by request from the laboratories of Franziska Denk (King's
145 College London) and Matt Ramer (the University of British Columbia).

146

147 **Surgical Procedures**

148 For the sciatic nerve crushes the animals were administered buprenorphine (0.02mg/kg;
149 Temgesic®) and ketoprofen (5mg/kg; Anafen®) subcutaneously for prophylactic analgesia.
150 Once anaesthetized with isoflurane (5% induction, 2-3% maintenance; Fresenius Kabi Canada
151 Ltd.), the sciatic nerve was exposed by blunt dissection and crushed for 15 seconds (thrice, 5
152 seconds each) with fine #5 forceps at the sciatic notch. For the brachial nerve crush the same
153 anesthetic and analgesic protocols were used. The distal brachial plexus was exposed in the

An ATF3^{cre} mouse for axotomy-induced genetic editing.

154 upper forelimb, the median radial, and ulnar nerves were crushed with fine forceps. Tamoxifen
155 (Sigma) was dissolved in wheat germ oil (Denk et al. 2015) and injected at concentration of
156 75mg/kg at the time of injury. Pure anti-estrogen ICI 182,780 (Tocris) was delivered by gavage
157 the day before, the day of, and the day after injury (20µg dissolved in sunflower oil). For the 2-
158 day regeneration assays the injury site was marked with forceps dipped in graphite
159 (ThermoFisher). For retrograde tracing, 1µl of 5% FluorogoldTM (Santa Cruz Biotechnologies)
160 dissolved in 50:50 DMSO:PBS (SigmaAldrich) was injected intraneurally immediately prior to
161 injury with a 10µl Hamilton syringe (SigmaAldrich).

162 Spinal hemisection was also carried out with the same anesthetic and analgesic protocols
163 outlined above. A midline incision was made over the lower cervical/upper thoracic spinal cord,
164 and the C8 and T1 laminae were removed. A 25-gauge needle was inserted dorso-ventrally at the
165 midline between the C8 and T1 spinal segments to allow relatively atraumatic entry of one blade
166 of a pair of microscissors. The cord was laterally transected with microscissors; after hemostasis
167 was established, the muscle and skin were closed in layers with sutures. Mice were killed seven
168 days later.

169

170 **Functional outcomes**

171 To investigate the following anatomical and functional recovery outcomes we employed a
172 transgenic line with only the *Atf3* and *Pten* alleles altered (i.e. without reporter to avoid potential
173 confounds associated with high tdTomato expression). Specifically, in the first set of experiments
174 we compared ATF3^{+/+}, ATF3^{+/-cre} and ATF3^{cre/cre} mice in order to determine similarities to
175 previous knockout models (e.g. Gey et al., 2016). In the second set we compared

An ATF3^{cre} mouse for axotomy-induced genetic editing.

176 ATF3^{+cre}:PTEN^{+/+} mice with ATF3^{+cre}:PTEN^{fl/fl} in order to compare axotomy-induced PTEN
177 deletion with virally-mediated PTEN deletion (Gallaher and Steward, 2018).

178

179 **Behavioural Testing**

180 Reflex withdrawal or crossed extension (i.e. a nocifensive response) upon strong toe pinch
181 was assessed in mice lightly anesthetized with 2% isoflurane. Upon loss of righting reflexes,
182 each animal was removed from the induction chamber and placed prone on a table. To confirm
183 light anesthesia, the base of a contralateral toe was pinched with curved serrated forceps. If there
184 was no initial response, the other toes on the same foot were pinched in succession until either a
185 response occurred, or there was an escape attempt. If a nocifensive response occurred, the
186 ipsilateral toes were pinched starting with the first and ending with the fifth digit. As mice are
187 prey species, they are prone to thanatosis (playing dead), and can suppress nocifensive
188 withdrawal as they emerge from anesthesia. As such, a contralateral toe was pinched again
189 following ipsilateral toe trials. An absence of a contralateral nocifensive response was almost
190 always followed within 5 seconds by escape, and so the test was repeated. The test was also
191 repeated if the mouse regained consciousness while the ipsilateral paw was being assessed. The
192 presence or absence of a response to each ipsilateral toe pinch was recorded. If pinch to a
193 particular toe elicited a response two days in a row, recovery was assigned to the first.

194 For the grasping assay the mouse was suspended upside-down from a wire cage lid and the
195 grasping ability of the hindpaw was assessed and scored. Scores were assigned using the
196 following semi-quantitative metric: undirected paw placement=0, directed paw placement=1,
197 occasional grasp=2, consistent grasp=3. Both tests were carried out every other day starting on
198 the third post-operative day until the experimental endpoint (day 28).

An ATF3^{cre} mouse for axotomy-induced genetic editing.

199

200 **Electromyography**

201 Four weeks following injury, mice were anesthetized with urethane (3g/kg in dH₂O), and
202 their sciatic nerves were exposed at mid-thigh. The nerves were bathed in paraffin oil and draped
203 across a pair of silver wire hook electrodes (anode-cathode distance: 1mm). EMG needle
204 electrodes were placed subcutaneously over the lateral aspect of the hindpaw; one at the
205 calcaneus, the other just proximal to the base of the 5th digit (over the abductor digiti minimi
206 muscles). The nerve stimulated with 200 microsecond square wave current pulses using a
207 stimulus generator (Master 9, A.M.P.I., Jerusalem, Israel) and stimulus isolator (A.M.P.I.).
208 Signals were amplified using a Dual Bio-amp connected to a 16 channel Powerlab
209 (ADInstruments, Colorado Springs, CO, USA). Signals were sampled at 40kHz, and filtered
210 using LabChart7 software. After establishing appropriate electrode polarity, current pulses were
211 delivered at increasing intensities until an EMG signal became apparent, and threshold current
212 was recorded. The maximum EMG signal was then obtained, and the latency and amplitude of
213 the first positive peaks were recorded.

214

215 **Tissue Processing**

216 Mice were transcardially perfused with phosphate buffered saline followed by 4%
217 paraformaldehyde (ThermoFisher). Once dissected, tissue was post-fixed overnight in 4%
218 paraformaldehyde, then overnight again in 20% sucrose (ThermoFisher) in 0.1M phosphate
219 buffer. The tissue was then frozen in CryomatrixTM (ThermoFisher) and sectioned at 20μm
220 (DRG & sciatic nerve) or 50-100μm (spinal cord). In some cases (Fig. 1), whole sympathetic or
221 sensory ganglia were stained and imaged. All sections were blocked in 10% normal donkey

An ATF3^{cre} mouse for axotomy-induced genetic editing.

222 serum with 0.2% Triton-X plus 0.02% sodium azide in PBS. Sections were incubated overnight
223 with primary antibodies: rabbit anti-ATF3 (1:400, Santa Cruz SC-188), rabbit anti-ATF3 (1:500,
224 Novus NBP 1-85816), rabbit anti-SCG10 (1:1000 Novus NBP 1-49461), rabbit anti-PTEN
225 (1:400m Cell Signaling 9188), and mouse anti-PTEN (1:200, Cell Signaling 14642). Sections
226 were incubated for 2 hours with the appropriate secondary antibodies at a concentration of
227 1:1000: AlexaFluor 488 donkey anti-rabbit (Invitrogen A21206), and AlexaFluor 488 donkey
228 anti-mouse (Jackson 715-545-151). Slides were cover-slipped with ProLongTM Gold with DAPI
229 (Invitrogen).

230

231 **Image Acquisition and Quantification**

232 All images were acquired with a Zeiss LSM 800 confocal microscope using Zen (Blue)
233 software. Recombination efficiency four days post-lesion was determined by dividing the
234 number of ATF3⁺-plus-tdtomato⁺ neuronal nuclei by the total number of ATF3⁺ neuronal nuclei.
235 The 16-day recombination efficiency was calculated by dividing the number of tracer-positive
236 neuron cell bodies by the total number of reporter-positive cell bodies. All image processing and
237 quantification was done using ImageJ (Fiji Version 2.0.0-rc-66/1.52b).

238 Both PTEN antibodies produced specific staining, but with high background, varying
239 depending on tissue examined (DRG and spinal cord). After comparing both antibodies across all
240 tissues, our analyses relied on the Cell Signaling 9188 antibody for the DRG images and the Cell
241 Signaling 14642 for the ventral root images. PTEN immunoreactivity in the DRG was quantified
242 by measuring the mean pixel intensity of the entire cell layer of the DRG. In the spinal cord,
243 PTEN immunoreactivity was weak in motoneurons, but intense in motor axons on either side of
244 the ventral root exit zones, and so we focused our attention there. PTEN immunoreactivity in

An ATF3^{cre} mouse for axotomy-induced genetic editing.

245 ventral root axons was determined by selecting for tdtomato⁺ axons and measuring the PTEN
246 intensity of each axon.

247 To determine the regeneration density and distance along the sciatic nerve one best 20μm-
248 thick section (i.e. lacking folds, bubbles or other sectioning artifacts) was selected for each
249 animal, which was then fully imaged (z-stack and tiled). The stack was orthogonally projected
250 into a single image through its entire depth. The images were then processed to generate binary
251 overlays. The average density of SCG10 immuno-positive axons along the width of the nerve
252 was measured and then averaged over 100μm increments.

253

254 **Statistics**

255 All statistical analyses were carried out using Prism 7 (Graph Pad). We used a one-way
256 ANOVA followed by Tukey's multiple comparison test to compare PTEN immunoreactivity
257 amongst DRGs (ipsilateral and contralateral from ATF3-CreERT2 mice with and without floxed
258 PTEN, Fig. 5). We used the Kolmogorov-Smirnov goodness-of-fit test to compare PTEN
259 immunoreactivity in tdtomato⁺ axons between ATF3-CreERT2 tdtomato reporter mice with and
260 without floxed PTEN (Fig. 5). Differences in axonal regeneration between ATF3-CreERT2 mice
261 with and without floxed PTEN were determined on cumulative axon densities over 2 mm
262 increments from the crush injury using either a one-way ANOVA followed by Dunnett's
263 multiple comparison test (three groups) or an un-paired two-tailed t-test (two groups). For toe
264 pinch, we compared proportions of animals with 5 sensate digits (i.e. complete nocifensive
265 recovery) over time following injury using a log-rank (Mantel-Cox) test. The same test was used
266 to compare proportions of animals which showed consistent grasping with the injured hindpaw.
267 For EMG data, we compared ipsilateral and contralateral values (Threshold, Latency,

An ATF3^{cre} mouse for axotomy-induced genetic editing.

268 Amplitude) within groups using paired t-tests. Because we used males and females (which differ
269 in size), for between-group comparisons we used unpaired t-tests on ipsilateral:contralateral
270 ratios.

271

272

An ATF3^{cre} mouse for axotomy-induced genetic editing.

273 **RESULTS**

274 **ATF3-Driven Injury-Induced Recombination**

275 The Novus ATF3 antibody labeled the injured wildtype mice (ATF3^{+/+}) ipsilateral DRG
276 neurons but did not label the same ipsilateral DRG neurons in the homozygous mutant mice
277 (ATF3^{cre/cre}) (Fig. 1A). However, the Santa Cruz antibody did label the injured ipsilateral DRG
278 neurons in the ATF3^{cre/cre} mice, suggesting that it is not specific to ATF3 but another, injury-
279 dependent protein as there was no neuronal labeling of any contralateral DRGs (Fig. 1A).

280 ATF3-driven recombination was exceedingly rare in the uninjured nervous system (Fig.
281 1B,C), although it was noted that uninjured recombination appeared to be more prevalent in
282 older mice (data not shown). Four days after peripheral nerve injury there was a robust tdtomato
283 signal in the neuronal cell bodies in axotomized DRGs, stellate (sympathetic) ganglia (Fig. 1B),
284 and ventral motor pools (Fig. 1C,D) in the ATF3^{+cre} Ai14 reporter mice without the
285 administration of tamoxifen. Tdtomato expression was only present in neurons, and only in those
286 with nuclear ATF3 immunopositivity (Fig. 1B, C).

287 ATF3 expression is maximal at 4 days post injury but declines in sensory and motoneurons
288 between 10 and 20 days (Tsuji et al 2000). In 4-day lesions we calculated the proportion of
289 ATF3-positive DRG and motor neurons that were also tdtomato positive (Fig. 1B, G). For 16-
290 day lesions we identified injured neurons by fluorogold labeling (injected at the time of injury),
291 and determined the proportion that were also tdtomato labeled (Fig. 1F, G). In the DRG,
292 recombination efficiencies were (mean \pm SEM) 53% \pm 2% (4d) and 76% \pm 3% (16d). For
293 motoneurons the efficiencies were 45% \pm 2% (4d) and 65% \pm 3% (16d). When the estrogen
294 receptor α antagonist (ICI) was administered the amount of neuronal recombination was
295 reduced by almost 50% (from 53% \pm 2% to 28 \pm 1%, $P < 0.05$, $n = 3$ mice per group, Fig. 1E),

An ATF3^{cre} mouse for axotomy-induced genetic editing.

296 demonstrating that recombination was due to leak of the CreERT2 construct into the nucleus as a
297 result of inadequate cytoplasmic anchoring.

298

299 **Figure 1.**

300

301 In the injured distal stump of the sciatic nerve the Novus ATF3 antibody showed a uniform
302 and punctate ATF3 signal that was attributable to white blood cells (Fig. 2A). When only the
303 secondary antibody was used the same signal was present and not localized to the nucleus of the
304 putative white blood cells indicating that the antibody signal was an artifact, and that there was
305 no ATF3 upregulation in the injured sciatic nerve (Fig. 2B).

306 In the uninjured sciatic nerve, long, spindle shaped cells that morphologically resemble
307 Remak Schwann cells (RSC) (Gomez-Sanchez et al 2017) were tdtomato+ and therefore had
308 expressed ATF3 at some point in their lifetime (Fig. 2C). Seven days after axotomy there was an
309 increased density of these tdtomato+ RSCs (Fig. 2D) although they were not positive for ATF3
310 immunolabeling. Upon closer inspection four days after injury we found multiple examples of
311 tdtomato+ RSCs undergoing all phases of mitosis (Fig. 2E) suggesting that the increased density
312 was not due to an injury induced upregulation of ATF3 but instead was the result of proliferation
313 of previously-labelled cells.

314

315 **Figure 2.**

316

317 **ATF3's Role in Peripheral Regeneration and Functional Recovery**

An ATF3^{cre} mouse for axotomy-induced genetic editing.

318 Before employing the ATF^{cre} line to edit the genes of injured neurons to manipulate the
319 regenerative response we first wanted to characterize the effect of losing one or both copies of
320 the *Atf3* allele. Since the Cre insert prematurely terminates the ATF3 coding sequence the
321 ATF3^{cre} allele is notionally non-functional.

322 To determine if loss of the *Atf3* allele attenuated functional recovery after PNI we
323 examined behavioural recovery up to 28 days following sciatic crush, and electromyographical
324 (EMG) activity at the experimental endpoint. We found that for both the pinching and grasping
325 assays that the ATF3^{cre/cre} group had significantly diminished functional recovery (p=0.0046 for
326 pinch, p=0.0189 for grasp) (Fig. 3A,B). The performance of ATF^{cre/+} mice was intermediate for
327 both assays (p=0.0012 for pinch, p=0.0049 for grasp) suggesting a gene dosage effect (the
328 amount of functional transcript affects the level of recovery).

329 In terminal EMG experiments we found that the ATF^{cre/cre} group had significantly longer
330 peak latencies (Fig. 3E) (p=0.0003), and smaller compound muscle action potentials (Fig. 3F)
331 (p=0.002) when comparing ipsilateral:contralateral ratios to the controls, indicating more
332 complete muscle reinnervation in ATF3^{+/+} mice. There were no differences in activation
333 thresholds (Fig. 3D). Surprisingly the ATF^{cre/+} group resembled the ATF^{cre/cre} group in EMG
334 measures, displayed significantly longer peak latencies (Fig. 3E) (p=0.008), and smaller
335 compound muscle action potentials (Fig. 3F) (p=0.04) when comparing ipsilateral:contralateral
336 ratios to the controls providing further evidence of a gene dosage effect.

337

338 **Figure 3.**

339

An ATF3^{cre} mouse for axotomy-induced genetic editing.

340 The above data unequivocally demonstrate delayed functional recovery (which can only be
341 attributable to regeneration of injured axons given the absence of ATF3 expression in uninjured
342 neurons) in ATF3-deficient mice. We then asked when differences in regeneration could be
343 discerned between genotypes anatomically. To this end we assayed axonal regeneration along
344 the sciatic nerve 2 and 3 days after crush by taking a single section (one that lacked sectioning
345 artifacts like tears or folds) and imaged through its full 20 μ m depth) for analysis. Two days after
346 sciatic nerve crush, cumulative axon density was not yet different between ATF^{+/+}, ATF^{cre/+}, and
347 ATF^{cre/cre} groups (Fig. 4A,B). Three days after sciatic nerve crush a significant difference was
348 detected in cumulative axonal density at 2-4mm distal to the injury site between ATF^{+/+} and
349 ATF^{cre/cre} groups (p=0.0200), and the ATF^{+/cre} group tested positive as a significant intermediary
350 between groups (p=0.0108) (Fig. 4C,D). These anatomical results further support our findings
351 that loss of one or both copies of the ATF3 allele diminishes regeneration after PNI.

352

353 **Figure 4.**

354

355 **ATF3-Driven Injury-Induced PTEN Knockdown**

356 To determine if the ATF3^{+/cre} line can excise floxed endogenous genes we crossed it to a
357 floxed *Pten* line, crushed the sciatic nerve, and measured PTEN expression 28 days post injury.
358 Three sections each from five animals were used for analysis. High background with both PTEN
359 antibodies rendered precise estimates of recombination efficiency difficult, but the antibody
360 labeled small-diameter DRG neurons, as reported previously by Gallaher & Steward (2018).
361 There was no reduction in PTEN immunoreactivity between the ipsilateral and contralateral
362 DRG cell layers in control animals (Fig. 5A) indicating that injury itself does not change PTEN

An ATF3^{cre} mouse for axotomy-induced genetic editing.

363 expression. For reasons unknown, but possibly due to the leaky Cre-ERT2 construct, there was a
364 significant difference in intensity measurements between genotypes on the contralateral
365 (uninjured) side. Nevertheless, there was a significant reduction in PTEN expression on the
366 ipsilateral side compared to the contralateral side of ATF3^{+cre} PTEN^{fl/fl} mice (p=0.0113)
367 indicating that ATF3 driven Cre expression successfully excises the PTEN gene (Fig. 5A,B). The
368 non-specific background PTEN antibody intensity was determined from sections from ATF3^{+/+}
369 PTEN^{fl/fl} mice in which PTEN-positive DRG neuronal somata were excluded from regions of
370 interest (i.e. the ROIs were the negative of the PTEN-positive neurons). PTEN immunoreactivity
371 in ATF3^{+cre} PTEN^{fl/fl} mice was no different from background.

372 Spinal motoneurons were weakly PTEN-immunoreactive, and although somata were less
373 readily identifiable if they were also tdTomato positive (Fig. 5C), background staining precluded
374 reliable analysis in the ventral horn. We therefore examined PTEN expression in the ipsilateral
375 ventral roots (which were intensely PTEN-immunoreactive on either side of the ventral root exit
376 zone) seven days after sciatic nerve crush in reporter mice with ATF3^{+cre} and PTEN^{fl/fl} or
377 PTEN^{+/+} alleles. Four control animals and three experimental animals were used (three sections
378 from each). We found that PTEN expression was significantly reduced (p<0.0001) in the axons
379 that also expressed tdTomato in the PTEN^{fl/fl} group compared to controls (Fig. 5D).

380

381 **Figure 5.**

382

383 **ATF3-Driven PTEN Excision Improved Functional Recovery**

384 To determine whether the ATF3^{+cre} driven *Pten* excision was robust enough to effect
385 enhanced functional recovery after PNI we examined behavioural recovery over a month

An ATF3^{cre} mouse for axotomy-induced genetic editing.

386 following sciatic crush, and electromyographical (EMG) activity at the experimental endpoint.
387 For behavioural analysis the control group had 14 animals in it and the experimental group had
388 9. There were no differences in sensory (pinch) or sensorimotor (grasping) assays between the
389 ATF3^{+cre} PTEN^{fl/fl} and control groups (Fig. 6A,B), as has been reported previously (Gallaher &
390 Steward, 2018).

391 In terminal EMG experiments, however, we found that the ATF3^{+cre} PTEN^{fl/fl} group had a
392 significantly lower EMG activation threshold (Fig. 6E) ($p < 0.0001$), shorter peak latencies (Fig.
393 6F) ($p = 0.040$), and larger compound muscle action potentials (Fig. 6G) ($p = 0.003$) when
394 comparing ipsilateral:contralateral ratios to the controls, indicating more complete muscle
395 reinnervation in mice lacking PTEN.

396

397 **Figure 6.**

398

399 Enhanced functional recovery in PTEN deficient mice implies more robust axonal regeneration.

400 We were again curious as to when axonal regeneration following ATF3-driven injury induced

401 *Pten* excision might be detected histologically following sciatic crush injury. Six animals were

402 used in each group and a single section (lacking sectioning artifacts, and imaged through its full

403 20 μ m depth) was taken for analysis. Two days after sciatic nerve crush, axon density plotted as a

404 function of distance was obviously increased in ATF3^{+cre} PTEN^{fl/fl} over that in ATF3^{+cre}

405 PTEN^{+/+} mice, and the cumulative density at 2 mm was statistically greater ($p = 0.0008$) (Fig. 7).

406 This demonstrates that the ATF3^{+cre} line is able to edit the genes of injured neurons with enough

407 efficacy to produce anatomical differences in regeneration.

408

An ATF3^{cre} mouse for axotomy-induced genetic editing.

409 **Figure 7.**

410

411 **ATF3-Driven Recombination After Central Nervous System Injury.**

412 After confirming that the ATF3^{cre} line is capable of efficient recombination that can
413 selectively edit genes the genes of injured neurons after PNI we wanted to determine if the same
414 line was applicable to CNS injury. Six ATF3^{cre/+}:Ai14 reporter mice underwent a C8/T1 lateral
415 spinal hemisection, were killed 7 days after injury, and recombination throughout the entire CNS
416 was characterized. In the spinal cord, several tracts were reliably labeled, these included putative
417 rubrospinal, raphespinal, reticulospinal, and vestibulospinal descending tracts (Fig. 8C,D).
418 Additionally, ascending neurons were tdtomato⁺; based on anatomical position these are likely
419 to be spinothalamic spinocerebellar neurons (Fig. 8E,F). In the cervical cord, rostral to the injury
420 site, there was a substantial amount of recombination in primary afferents innervating the dorsal
421 horn (Fig. 8C). Four deep brain nuclei were consistently reporter-positive, these were the
422 rubrospinal, reticulospinal, vestibulospinal, and paraventricular hypothalamic nuclei (Fig 9A-E).
423 There were examples of ATF3 immunolabeled and tdtomato positive neurons in each of these
424 nuclei (Fig 9F).

425

426 **Figure 8.**

427 **Figure 9.**

428

429 **DISCUSSION**

430 The expression of Cre recombinase has for the most part been restricted to either
431 developmentally distinct subpopulations of cells *via* its insertion under specific promoters or to

An ATF3^{cre} mouse for axotomy-induced genetic editing.

432 distinct physical regions by viral transfection. Selective cellular genetic modification of neurons
433 based upon functional state is an attractive and important refinement to this approach. Guenther
434 et al. (2013), for example used a genetic labeling technique controlled by neuronal activity. In
435 this case recombination was driven by promoters for the immediate-early genes Fos and Arc,
436 upregulated as part of the “excitation-transcription” neuronal response to synaptic activity
437 initiated by CREB phosphorylation. Here we present a novel transgenic mouse line that
438 expresses Cre only once peripherally-projecting neurons have been axotomized by inserting its
439 construct into the native ATF3 locus. We demonstrate a substantial amount of recombination
440 (~50% by 4d post-injury, rising to ~65-80% by 16d) in injured sensory, motor, and sympathetic
441 neurons that is selective to axotomy. This injury-dependent Cre expression is restricted to the
442 neurons that have been axotomized, is rare in uninjured controls, and absent in peripheral glial
443 cells. Furthermore, we show that axotomy-induced Cre expression can excise floxed genes with
444 sufficient efficacy to significantly effect anatomical regeneration and functional recovery.

445 It is important to note that despite the Cre recombinase being anchored to a mutated
446 estrogen receptor (ERT2) we have achieved significant recombination without the administration
447 of tamoxifen. This can be attributed to the “leakiness” of the ERT2 construct where the ERT2
448 protein overwhelms its cytoplasmic anchor and translocates to the nucleus without tamoxifen (or
449 its metabolites) binding. The high degree of tamoxifen-independent recombination we report is
450 likely driven by massive upregulation of ATF3 in the PNS after injury: the *Atf3* gene (and hence
451 Cre-ERT2) is highly transcribed once the neuron is axotomized, and there is a greater likelihood
452 of ERT2 leak and subsequent recombination. Reduction of recombination by ICI 182,780 (Fig.
453 1) provides an opportunity to titrate recombination due to leakiness.

An ATF3^{cre} mouse for axotomy-induced genetic editing.

454 We did not use tamoxifen to improve the recombination efficiency of the model, as it has
455 been previously reported that tamoxifen administration, at the standard dose of 75mg/kg,
456 upregulates ATF3 without injury (Denk et al 2015). Notionally it is possible that a lower dose of
457 tamoxifen would not induce ATF3 expression, but would still improve the recombination
458 efficiency after injury, although this dose has yet to be determined. Regardless, the efficiencies
459 achieved in this report due to ERT2 leak remain sufficient to excise *Pten* and significantly
460 improve anatomical regeneration and functional recovery.

461 The potential utility of our model is strengthened by similarities to previous manipulations
462 using different techniques. A study by Gallaher & Steward (2018) investigated the effect of *Pten*
463 deletion following axotomy in the sensory neurons that innervate the sciatic nerve. They excised
464 *Pten* through a more traditional intraganglionic injection of an AAV Cre vector into the L4 and
465 L5 DRG. Their study and ours agree on three key results: 1) PTEN immunohistochemistry
466 preferentially labels small diameter sensory neurons, 2) PTEN deletion increased axonal
467 regeneration along the sciatic nerve three days after axotomy, and 3) PTEN deletion after sciatic
468 nerve crush did not significantly improve sensory functional recovery. The ATF3-CreERT2 line
469 has several distinct advantages over more traditional Cre delivery models; the technical viral
470 transfection setup is not necessary and Cre can be expressed in neuronal populations that may
471 not be amenable to local injection. Moreover, the ATF3-ERT2 line allows for the selective
472 editing of only injured neurons where a viral Cre transfection does not preclude the possibility of
473 Cre expression in uninjured neurons.

474 Using a homozygous knockin (i.e. null mutant), we tested the validity of two reported
475 ATF3 specific polyclonal antibodies: Novus (NBP 1-85816) and Santa Cruz (C-19). ATF3 signal
476 was expectedly absent in the ATF3 null ipsilateral DRG after axotomy when using the Novus

An ATF3^{cre} mouse for axotomy-induced genetic editing.

477 antibody. However, signal was still present in both the control and ATF3 null ipsilateral (but not
478 contralateral) DRG when tested with the Santa Cruz antibody suggesting that is not specific to
479 ATF3, but likely another injury-dependent protein. This could call into question some of the
480 conclusions made by the over 150 articles that have utilized this antibody. We then used the
481 Novus ATF3 antibody to investigate ATF3 expression in the injured sciatic nerve. Despite the
482 appearance of putative ATF3 upregulation, we were able to determine that this signal was
483 restricted to white blood cells, non-nuclear, and in fact due to background fluorescence.
484 Clements et al. (2017) reports Schwann cell ATF3 mRNA expression in the uninjured sciatic
485 nerve which is then reduced upon injury, which appears to contradict our observations of a lack
486 of ATF3 driven recombination in normal Schwann cells but supports our finding of a lack of
487 injury dependent glial cell ATF3 expression. To obtain these data the Schwann cells needed to be
488 dissociated, purified, and then sorted before sequencing. Given ATF3's role as a stress response
489 immediate early gene it is certainly plausible that this baseline ATF3 expression is due to the
490 FACS process and not in fact expressed in the *in vitro* uninjured nerve – this has indeed proven
491 to be an issue in other cell types, such as muscle (van den Brink et al 2017). Histological
492 evidence of ATF3 mRNA upregulation following nerve injury is also unconvincing (Hunt et al
493 2004). We therefore conclude that ATF3 is not upregulated in peripheral glia after injury cells,
494 contrary to previous reports. This finding further strengthens the usefulness of the model as any
495 axotomy-dependent Cre upregulation is restricted to neuronal populations.

496 Tdtomato-positive Remak Schwann cells (RSCs) increased in density following sciatic
497 nerve injury. RSCs are a subtype of Schwann cell that are non-myelinating but still ensheath
498 small caliber axons to form Remak bundles (Harty & Monk, 2017). Gomez-Sanchez et al (2017)
499 characterized this subtype of Schwann cells using sporadic permanent fluorophore labelling.

An ATF3^{cre} mouse for axotomy-induced genetic editing.

500 These cells are spindle shaped, can be branched, and are approximately 250um in length; all of
501 which are characteristics of the sciatic nerve cells found to undergo injury-independent
502 recombination in the ATF3^{cre} Ai14 reporter line. The absence of ATF3 immunoreactivity in
503 these cells, along with the high numbers of RSCs that can be observed undergoing mitosis four
504 days after injury show that their increase in density is due to cellular division rather than injury-
505 induced ATF3-cre-mediated recombination.

506 The ATF3^{cre/cre} null mutant also allowed us to test the effect of a loss of ATF3 function in
507 peripheral nervous system regeneration early after injury. While we found no significant
508 differences between the groups in axonal regeneration along the sciatic nerve at the two-day time
509 point, we did find a statistically significant functional deficit of both ATF3-deficient groups in
510 both our behavioural and electromyographical assays. Despite being a standard timepoint for this
511 type of analysis, the lack of significantly different 2-day axonal regeneration along the sciatic
512 nerve could be because the axons have not had sufficient time to differentially regenerate enough
513 to produce a measurable difference. This supports previous work done by Gey et al (2016) who
514 found attenuated regeneration after facial nerve axotomy in ATF3 null mice. Gey et al (2016)
515 also showed that when DRG neurons were cultured in the presence of NGF, any differences in
516 outgrowth between wild-type and knockout neurons ATF3 were abolished. NGF is produced
517 early on in the distal transected nerve (Heumann et al 1987), and this early abundance may
518 compensate for any ATF3-mediated regenerative differences. By three days post-injury,
519 however, a clear difference between ATF3^{+/+} and ATF3^{cre/cre} mice had emerged, along with
520 evidence again for haploinsufficiency (the intermediate position of ATF3^{+/cre} mice). To our
521 knowledge, this is the first evidence that a loss of ATF3 mitigates functional recovery after
522 injury.

An ATF3^{cre} mouse for axotomy-induced genetic editing.

523 Interestingly the existing literature suggests that ATF3 heterozygotes are haplosufficient
524 (Gey et al 2016) which is contrary to our findings of a gene dosage effect. The fact that the
525 amount of ATF3 transcript affects the functional outcome after peripheral axotomy might seem
526 surprising given how drastically ATF3 is upregulated in neurons after injury. However, given
527 that ATF3 is a bZIP transcription factor that dimerizes with itself or other bZIP transcription
528 factors to affect transcription, it is conceptually possible that the binding affinity for the ATF3
529 dimerization pair responsible for improving regeneration is low and therefore many copies of
530 ATF3 must be produced for its pro-regenerative effect. Recent work done by Rodriguez-
531 Martinez et al 2017 exemplified this by showing that ATF3's DNA binding site preference to be
532 highly dependent on its bZIP dimerization.

533 ATF3 gene dosage effects (i.e. partial function in hemizygous mice) should not be an
534 impediment to investigations of functions of other (floxed) genes or sequences provided the
535 appropriate controls are used. There is simply a new baseline upon which other genetic
536 manipulations (using ATF3-Cre-driven excision of floxed gene "X") can be evaluated. For this
537 reason it is important that any investigation of the function of gene X compares ATF3^{+cre}:X^{+/+}
538 with ATF3^{+cre}:X^{fl/fl} (or ATF3^{+cre}:X^{+fl}, for investigating possible haploinsufficiency of X), as we
539 have done here substituting "X" with "PTEN".

540 ATF3 is not only upregulated after PNI but also after CNS trauma including spinal cord
541 injury (Huang et al 2007), albeit usually meagerly and/or transiently, rendering expression
542 patterns difficult to reveal (reviewed in Hunt et al., 2012). As such we wanted to determine if
543 CNS neurons could be accessed genetically via ATF3-cre-mediated recombination after a lateral
544 spinal cord hemisection. We observed consistent recombination in four deep brain nuclei
545 (rubrospinal, reticulospinal, vestibulospinal, and hypothalamic) and their projecting axons and in

An ATF3^{cre} mouse for axotomy-induced genetic editing.

546 at least two putative ascending tracts (spinocerebellar and spinothalamic). There was no
547 recombination observed in the injured corticospinal tract, but this is not surprising given that it
548 takes intracortical axotomy to induce ATF3 in corticospinal neurons (Mason et al 2003): the
549 magnitude of upregulation of regeneration associated genes (of which ATF3 is) have been
550 documented to be dependent on the distance from the axon transection to the soma (Fernandes et
551 al 1999).

552 The mammalian PNS is able to regenerate after injury, unlike the CNS where regeneration
553 does not occur. This positions the PNS as an excellent model for study to better understand what
554 is necessary for mammalian neuronal regeneration. The ability to edit the genes of injured
555 neurons and further dissect what is necessary and/or sufficient to produce this regeneration is of
556 obvious value, and is now possible with the ATF^{cre} transgenic line. ATF3 is also expressed in
557 injured neurons after spinal cord injury (Huang et al 2007, Wang et al 2015, Darlot et al 2017),
558 traumatic brain injury (Forstner et al 2018), and ischemic stroke (Song et al 2011), making the
559 line useful to scientists interested in the neuronal response to each of those pathologies. Mice are
560 available by direct request to Dr. Franziska Denk (King's College London), or Dr. Matt Ramer
561 (the University of British Columbia).

562

An ATF3^{cre} mouse for axotomy-induced genetic editing.

563 **REFERENCES**

564

565 Agarwal N, Offermanns S, Kuner R (2004) Conditional gene deletion in primary nociceptive
566 neurons of trigeminal ganglia and dorsal root ganglia. *Genesis* 38:122–129.

567 Broude E, McAtee M, Kelley M., Bregman B (1997) c-Jun Expression in Adult Rat Dorsal Root
568 Ganglion Neurons: Differential Response after Central or Peripheral Axotomy. *Experimental*
569 *Neurology* 148:367–377.

570 Clausen BE, Burkhardt C, Reith W, Renkawitz R, Förster I (1999) Conditional gene targeting in
571 macrophages and granulocytes using LysMcre mice. *Transgenic Research* 8:265–277.

572 Clements MP, Byrne E, Guerrero LFC, Cattin A-L, Zakka L, Ashraf A, Burden JJ, Khadayate S,
573 Lloyd AC, Marguerat S (2017) The wound microenvironment reprograms Schwann cells to
574 invasive mesenchymal-like cells to drive peripheral nerve regeneration. *Neuron* 96:98-114.

575 Darlot F, Vinit S, Matarazzo V, Kastner A (2017) Sustained cell body reactivity and loss of
576 NeuN in a subset of axotomized bulbospinal neurons after a chronic high cervical spinal cord
577 injury. *Eur J Neurosci* 46:2729-2745.

578 Denk F, Ramer LM, Erskine EL, Nassar MA, Bogdanov Y, Signore M, Wood JN, McMahon
579 SB, Ramer MS (2015) Tamoxifen induces cellular stress in the nervous system by inhibiting
580 cholesterol synthesis. *Acta Neuropathol Commun* 3:74.

581 Fernandes KJ, Fan DP, Tsui BJ, Cassar SL, Tetzlaff W (1999) Influence of the axotomy to cell
582 body distance in rat rubrospinal and spinal motoneurons: differential regulation of GAP-43,
583 tubulins, and neurofilament-M. *The Journal of comparative neurology* 414:495–510.

584 Förstner P, Rehman R, Anastasiadou S, Haffner-Luntzer M, Sinske D, Ignatius A, Roselli F,
585 Knöll B (2018a) Neuroinflammation after Traumatic Brain Injury Is Enhanced in Activating
586 Transcription Factor 3 Mutant Mice. *Journal of Neurotrauma* 35:2317–2329.

An ATF3^{cre} mouse for axotomy-induced genetic editing.

- 587 Gallaher ZR, Steward O (2018) Modest enhancement of sensory axon regeneration in the sciatic
588 nerve with conditional co-deletion of PTEN and SOCS3 in the dorsal root ganglia of adult mice.
589 *Experimental Neurology* 303:120–133.
- 590 Gey M, Wanner R, Schilling C, Pedro MT, Sinske D, Knoll B (2016) Atf3 mutant mice show
591 reduced axon regeneration and impaired regeneration-associated gene induction after peripheral
592 nerve injury. *Open Biol* 6.
- 593 Gomez-Sanchez JA, Pilch KS, Van Der Lans M, Fazal SV, Benito C, Wagstaff LJ, Mirsky R,
594 Jessen KR (2017) Development/Plasticity/Repair After Nerve Injury, Lineage Tracing Shows
595 That Myelin and Remak Schwann Cells Elongate Extensively and Branch to Form Repair
596 Schwann Cells, Which Shorten Radically on Remyelination. *Journal of Neuroscience*
597 13;37(37):9086-9099.
- 598 Guenther CJ, Miyamichi K, Yang HH, Heller HC, Luo L (2013) Permanent genetic access to
599 transiently active neurons via TRAP: targeted recombination in active populations. *Neuron*
600 78:773-784.
- 601 Harty BL, Monk KR (2017) Unwrapping the unappreciated: recent progress in Remak Schwann
602 cell biology. *Current Opinion in Neurobiology* 47:131–137.
- 603 Hawthorne AL, Hu H, Kundu B, Steinmetz MP, Wylie CJ, Deneris ES, Silver J (2011) The
604 unusual response of serotonergic neurons after CNS Injury: lack of axonal dieback and enhanced
605 sprouting within the inhibitory environment of the glial scar. *The Journal of neuroscience*
606 31:5605–16.
- 607 Hayashi S, McMahon AP (2002) Efficient Recombination in Diverse Tissues by a Tamoxifen-
608 Inducible Form of Cre: A Tool for Temporally Regulated Gene Activation/Inactivation in the
609 Mouse. *Developmental Biology* 244:305–318.

An ATF3^{cre} mouse for axotomy-induced genetic editing.

- 610 Huang WL, George KJ, Ibba V, Liu MC, Averill S, Quartu M, Hamlyn PJ, Priestley JV (2007)
611 The characteristics of neuronal injury in a static compression model of spinal cord injury in adult
612 rats. *European Journal of Neuroscience* 25:362–372.
- 613 Hunt D, Hossain-Ibrahim K, Mason MR, Coffin RS, Lieberman AR, Winterbottom J, Anderson
614 PN (2004) ATF3 upregulation in glia during Wallerian degeneration: differential expression in
615 peripheral nerves and CNS white matter. *BMC neuroscience* 5:9.
- 616 Hunt D, Raivich G, Anderson PN (2012) Activating Transcription Factor 3 and the Nervous
617 System. *Front Mol Neurosci* 5.
- 618 Indra AK, Warot X, Brocard J, Bornert J-M, Xiao J-H, Chambon P, Metzger D (1999)
619 Temporally-controlled site-specific mutagenesis in the basal layer of the epidermis: comparison
620 of the recombinase activity of the tamoxifen-inducible Cre-ERT and Cre-ERT2 recombinases.
621 *Nucleic Acids Research* 27:4324–4327.
- 622 Kang H, Tian L, Thompson W (2003) Terminal Schwann cells guide the reinnervation of muscle
623 after nerve injury. *Journal of Neurocytology* 32:975–985.
- 624 Kouyoumdjian JA (2006) Peripheral nerve injuries: a retrospective survey of 456 cases. *Muscle*
625 *Nerve* 34:785-788.
- 626 Leone DP, Genoud S, Atanasoski S, Grausenburger R, Berger P, Metzger D, Macklin WB,
627 Chambon P, Suter U (2003) Tamoxifen-inducible glia-specific Cre mice for somatic mutagenesis
628 in oligodendrocytes and Schwann cells. *Molecular and Cellular Neuroscience* 22:430–440.
- 629 Lesche R, Groszer M, Gao J, Wang Y, Messing A, Sun H, Liu X, Wu H (2002) Cre/loxP-
630 mediated inactivation of the murine Pten tumor suppressor gene. *Genesis* 32:148–149.
- 631 Liang G, Wolfgang CD, Chen BP, Chen TH, Hai T (1996) ATF3 gene. Genomic organization,
632 promoter, and regulation. *The Journal of biological chemistry* 271:1695–701.

An ATF3^{cre} mouse for axotomy-induced genetic editing.

- 633 Liu K, Lu Y, Lee JK, Samara R, Willenberg R, Sears-Kraxberger I, Tedeschi A, Park KK, Jin D,
634 Cai B, Xu B, Connolly L, Steward O, Zheng B, He Z (2010) PTEN deletion enhances the
635 regenerative ability of adult corticospinal neurons. *Nature neuroscience* 13:1075–81.
- 636 Liu Q, Trotter J, Zhang J, Peters MM, Cheng H, Bao J, Han X, Weeber EJ, Bu G (2010)
637 Neurobiology of Disease Neuronal LRP1 Knockout in Adult Mice Leads to Impaired Brain
638 Lipid Metabolism and Progressive, Age-Dependent Synapse Loss and Neurodegeneration.
639 *Journal of Neuroscience* 30(50):17068-78
- 640 Madisen L, Zwingman TA, Sunkin SM, Oh SW, Zariwala HA, Gu H, Ng LL, Palmiter RD,
641 Hawrylycz MJ, Jones AR, Lein ES, Zeng H (2010) A robust and high-throughput Cre reporting
642 and characterization system for the whole mouse brain. *Nature Neuroscience* 13:133–140.
- 643 Mason MRJ, Lieberman AR, Anderson PN (2003) Corticospinal neurons up-regulate a range of
644 growth-associated genes following intracortical, but not spinal, axotomy. *The European journal*
645 *of neuroscience* 18:789–802.
- 646 Nishida A, Furukawa A, Koike C, Tano Y, Aizawa S, Matsuo I, Furukawa T (2003) Otx2
647 homeobox gene controls retinal photoreceptor cell fate and pineal gland development. *Nature*
648 *Neuroscience* 6:1255–1263.
- 649 Noble J, Munro CA, Prasad VS, Midha R (1998) Analysis of upper and lower extremity
650 peripheral nerve injuries in a population of patients with multiple injuries. *J Trauma* 45:116-122.
- 651 Park KK, Liu K, Hu Y, Smith PD, Wang C, Cai B, Xu B, Connolly L, Kramvis I, Sahin M, He Z
652 (2008) Promoting Axon Regeneration in the Adult CNS by Modulation of the PTEN/mTOR
653 Pathway. *Science* 322:963–966.
- 654 Rodríguez-Martínez JA, Reinke AW, Bhimsaria D, Keating AE, Ansari AZ (2017)
655 Combinatorial bZIP dimers display complex DNA-binding specificity landscapes. *eLife*.

An ATF3^{cre} mouse for axotomy-induced genetic editing.

- 656 Sainsbury A, Schwarzer C, Couzens M, Fetissov S, Furtinger S, Jenkins A, Cox HM, Sperk G,
657 Hökfelt T, Herzog H (2002) Important role of hypothalamic Y2 receptors in body weight
658 regulation revealed in conditional knockout mice. *Proceedings of the National Academy of*
659 *Sciences of the United States of America* 99:8938–43.
- 660 Seijffers R, Mills CD, Woolf CJ (2007) ATF3 increases the intrinsic growth state of DRG
661 neurons to enhance peripheral nerve regeneration. *J Neurosci* 27:7911-7920.
- 662 Song D-Y, Oh K-M, Yu H-N, Park C-R, Woo R-S, Jung S-S, Baik T-K (2011) Role of activating
663 transcription factor 3 in ischemic penumbra region following transient middle cerebral artery
664 occlusion and reperfusion injury. *Neuroscience Research* 70:428–434.
- 665 Stambolic V, Suzuki A, de la Pompa JL, Brothers GM, Mirtsos C, Sasaki T, Ruland J, Penninger
666 JM, Siderovski DP, Mak TW (1998) Negative regulation of PKB/Akt-dependent cell survival by
667 the tumor suppressor PTEN. *Cell* 95:29-39.
- 668 Sun F, Park KK, Belin S, Wang D, Lu T, Chen G, Zhang K, Yeung C, Feng G, Yankner BA, He
669 Z (2011) Sustained axon regeneration induced by co-deletion of PTEN and SOCS3. *Nature*
670 480:372-375.
- 671 Tetzlaff W, Alexander SW, Miller FD, Bisby MA (1991) Response of facial and rubrospinal
672 neurons to axotomy: changes in mRNA expression for cytoskeletal proteins and GAP-43. *The*
673 *Journal of Neuroscience* 11:2528–44.
- 674 Tsujino H, Kondo E, Fukuoka T, Dai Y, Tokunaga A, Miki K, Yonenobu K, Ochi T, Noguchi K
675 (2000) Activating transcription factor 3 (ATF3) induction by axotomy in sensory and
676 motoneurons: A novel neuronal marker of nerve injury. *Molecular and cellular neurosciences*
677 15:170–82..

An ATF3^{cre} mouse for axotomy-induced genetic editing.

- 678 van den Brink SC, Sage F, Vértesy A, Spanjaard B, Peterson-Maduro J, Baron CS, Robin C, Van
679 Oudenaarden A (2017) Single-cell sequencing reveals dissociation-induced gene expression in
680 tissue subpopulations. *Nature methods* 14:935.
- 681 Wagner K-U, Wall RJ, St-Onge L, Gruss P, Wynshaw-Boris A, Garrett L, Li M, Furth PA,
682 Hennighausen L (1997) Cre-mediated gene deletion in the mammary gland. *Nucleic Acids*
683 *Research* 25:4323–4330.
- 684 Wang W, Liu R, Xu Z, Niu X, Mao Z, Meng Q, Cao X (2015) Further insight into molecular
685 mechanism underlying thoracic spinal cord injury using bioinformatics methods. *Molecular*
686 *Medicine Reports* 12:7851–7858.
- 687

An ATF3^{cre} mouse for axotomy-induced genetic editing.

688 **Figure Legends**

689 **Figure 1. Axotomy-induced recombination in peripherally-projecting neurons. A,**
690 Validation of an ATF3-specific antibody. The Novus antibody (NBP1-85816) produces a
691 positive signal in nuclei of axotomized sensory neurons in ATF3^{+/+} mice, but not ATF3^{cre/cre}
692 mice. Note that the Santa Cruz antibody (C-19) labels neuronal nuclei in the latter (inset),
693 indicating non-specific staining. **B, C,** Axotomy induced reporter expression in sensory (DRG),
694 sympathetic (stellate ganglion, SG), and motoneurons four days post-injury. **D,** Reporter
695 expression in sensory axons and motoneurons one week post-injury. **E,** Preventing CreERT2
696 translocation from cytoplasm to nucleus with ICI 182,780 reduces recombination in ATF3⁺ cells
697 (by ~50%). **F,** Recombination efficiency 16 days post-injury was calculated by expressing the
698 proportion of tracer-filled somata (labeled at the time of injury) that were also reporter
699 (tdtomato)-positive. **G,** Recombination efficiencies at 4d and 16d post injury (n=3 for each
700 timepoint) for DRG and motoneurons. Images in panels **A, B,** and **E** were taken from whole
701 mounts, those in **C, D,** and **F** from cryosections.

702

703 **Figure 2. Axotomy does not induce ATF3 in Schwann cells. A,** Cryosections from injured
704 DRG (inset) and distal sciatic nerve from the same mouse processed for ATF3
705 immunohistochemistry (Novus NBP1-85816). **B,** Punctate staining in the nerve proved to be
706 non-specific fluorescence of leukocytes (note non-nuclear signal in the absence of primary
707 antibody). **C,** In intact sciatic nerves, cells morphologically identical to Remak cells had at some
708 point undergone recombination. **D,** Following injury, their numbers increased. **E,** This was
709 attributable to their proliferation in the injured nerve (as opposed to ATF3 induction and
710 subsequent recombination).

An ATF3^{cre} mouse for axotomy-induced genetic editing.

711

712 **Figure 3. Loss of ATF3 function delays functional recovery following sciatic nerve crush.**

713 **A,B**, The rate of functional recovery (nocifensive reflex withdrawal to a toe pinch and presence
714 of any grasping ability) was reduced in mice lacking both wild-type ATF3 alleles (log rank
715 Mantel-Cox test). Haploinsufficiency was also suggested by the statistically-significant trend
716 from wild-type to homozygous knock-in (log rank Mantel-Cox test), n = 7, 9, & 8 for ATF3^{+/+},
717 ATF3^{+/-}, & ATF3^{-/-} respectively. **C**, Representative EMG traces from ipsilateral and contralateral
718 sides of an ATF3^{+/+} mouse 28 days post sciatic nerve crush, and composite traces from 7
719 ATF3^{+/+} mice and 7 ATF3^{cre/cre} mice. **D**, EMG thresholds did not differ between genotypes
720 (paired t-test). **E, F**, While absolute latencies and amplitudes did not differ between genotypes
721 (paired t-test), their ipsilateral:contralateral ratios (correcting for mouse size) indicated reduced
722 conduction velocity (**E**) and extent of reinnervation (**F**) in mice lacking one or both wild-type
723 ATF3 alleles (unpaired t-test), n = 6, 7, & 6 for ATF3^{+/+}, ATF3^{+/-}, & ATF3^{-/-} respectively.

724

725 **Figure 4. Loss of ATF3 function modestly reduces axonal regeneration following sciatic**

726 **nerve crush. A, B**, There was no difference in axonal regeneration 2 days following injury
727 between ATF3^{+/+}, ATF3^{+/cre} and ATF3^{cre/cre} mice (n=7, 6, & 6 respectively, groups were
728 compared with a one-way ANOVA on cumulative densities). **C, D**, ATF3^{cre/cre} mice exhibited
729 significantly diminished axonal regeneration 3 days following injury 2-4mm distal to the injury
730 compared to ATF3^{+/+} mice (n=5 for both groups, One-way ANOVA followed by Dunnett's
731 multiple comparison test). The hemizygous group (n=4) tested positive as a significant
732 intermediary between both control and ATF3 null groups (post-hoc test for trend). Dotted line
733 indicates distal border of crush site, 500µm from the edge of the block. Scale bars: 500µm.

An ATF3^{cre} mouse for axotomy-induced genetic editing.

734

735 **Figure 5. Axotomy-induced PTEN deletion in sensory and motoneurons. A, B,** Axotomy
736 results in significant loss of PTEN expression in the DRG. Arrows in **A** indicate small PTEN-
737 positive DRG neurons. The PTEN antibody results in high background staining in all animals, to
738 which PTEN immunoreactivity is reduced in axotomized DRGs of ATF3^{+cre}:PTEN^{fl/fl} mice (**B**)
739 (one-way ANOVA followed by Dunnett's multiple comparison test, n=5 for both groups). **C,**
740 PTEN immunoreactivity is weak in all motoneurons, rendering difficult confirmation of
741 axotomy-induced knockdown. However, ventral root (VR, large arrow) axons close to the
742 ventral root exit zone were intensely immunopositive, single arrows indicate axons that were
743 both tdtomato and PTEN positive, whereas double arrows indicate recombination without PTEN
744 immunoreactivity. In sections of ventral roots we were able to demonstrate a significant decrease
745 in PTEN immunoreactivity in tdtomato-positive axons (**D**) (Kolmogorov-Smirnov goodness of
746 fit test), n=4 & n=3 for ATF3^{+cre}:PTEN^{+/+} & ATF3^{+cre}:PTEN^{fl/fl} respectively. Scale bars: A,
747 50µm; C, 100µm; E, 10µm.

748

749 **Figure 6. Axotomy-induced PTEN deletion and improves functional recovery following**
750 **sciatic nerve crush. A,B,** While there was no difference in recovery of reflex nociception or
751 grasping in mice with floxed PTEN alleles (log rank Matel-Cox test, n=14 & n=9 for
752 ATF3^{+cre}:PTEN^{+/+} & ATF3^{+cre}:PTEN^{fl/fl} respectively), EMG responses (**C-G**) indicated
753 enhanced recovery of neuromuscular function. **C, D,** Representative EMG traces from ipsilateral
754 and contralateral sides of an ATF3^{+cre}:PTEN^{+/+} mouse 28 days post sciatic nerve crush (**C**), and
755 composite traces from 8 ATF3^{+cre}:PTEN^{+/+} mice and 6 ATF3^{cre/cre}:PTEN^{fl/fl} mice. **E-G,**
756 ipsilateral:contralateral ratios of EMG thresholds (**E**), peak EMG latencies (**F**) and maximum

An ATF3^{cre} mouse for axotomy-induced genetic editing.

757 CMAP amplitudes (**G**) all indicated more complete muscle reinnervation 28 days post injury.
758 n=8 & n=6 for ATF3^{+cre}:PTEN^{+/+} & ATF3^{+cre}:PTEN^{fl/fl} respectively, averages were compared
759 using paired t-tests and ipsilateral:contralateral ratios with unpaired t-tests.

760

761 **Figure 7. Axotomy-induced PTEN deletion and anatomical regeneration following sciatic**
762 **nerve crush. A, B,** Axonal regeneration 2 days subsequent to sciatic nerve crush (dotted line)
763 was significantly enhanced in ATF3^{+cre}:PTEN^{fl/fl} mice. In **C**, bar graphs represent the cumulative
764 density of SCG10 immunoreactivity from 0 μm (the distal extent of the crush site) to 2000 μm .
765 n=6 for both groups and cumulative densities were compared using an unpaired t-test. Scale bars:
766 500 μm .

767

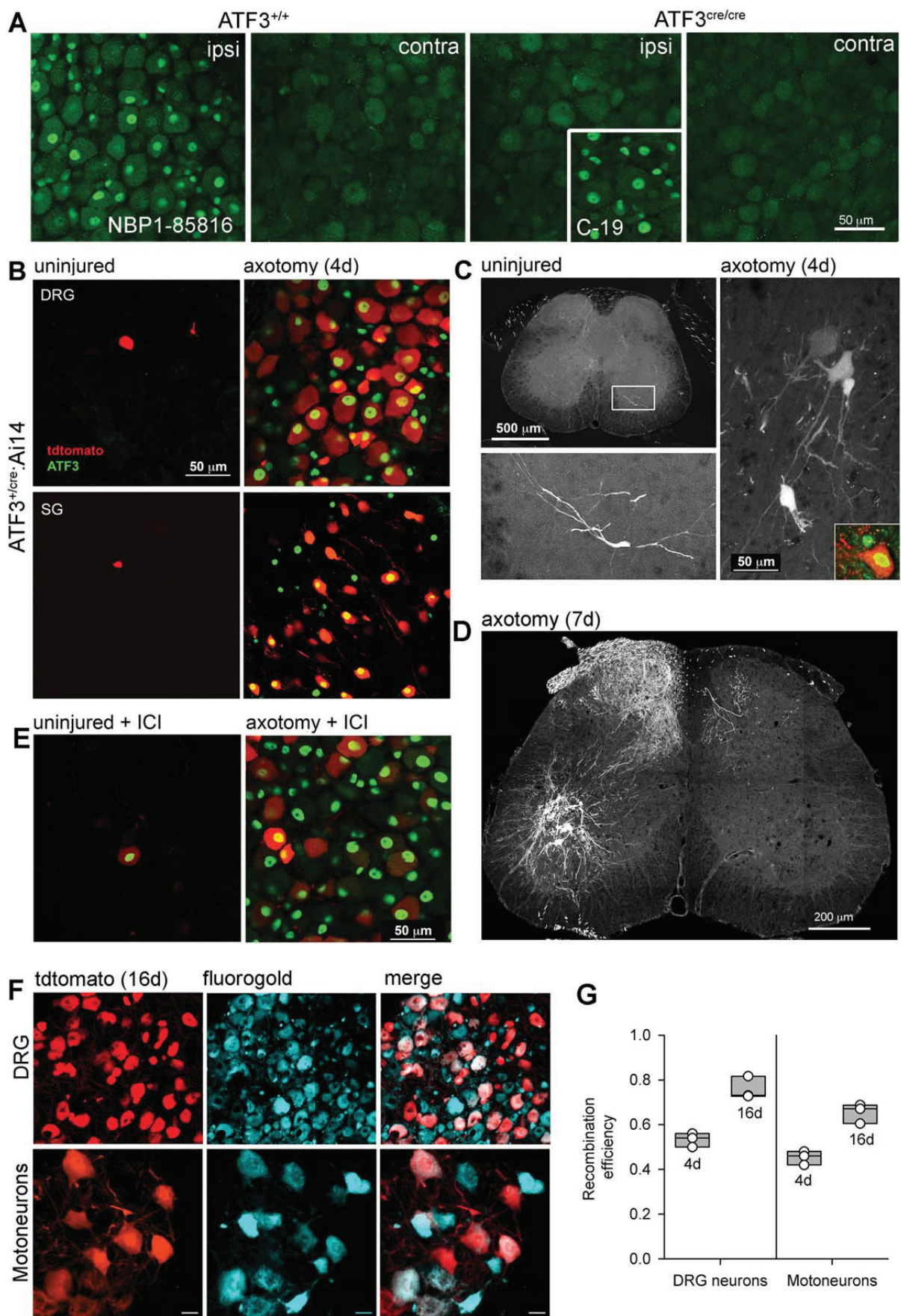
768 **Figure 8. Axotomy-induced recombination one week following spinal hemisection: spinal**
769 **cord. A,** Two examples of the injury site from separate animals in longitudinal section. Insets
770 show consistently-recombining ipsilaterally-projecting neurons near Clarke's column below the
771 injury. **B,** Cartoon of transverse section of the hemisected spinal cord illustrating relative
772 positions of positionally and morphologically distinguishable recombined neurons (coloured dots
773 correspond to examples in **C-F**). **C,** Examples of recombination after injury in cervical (top left),
774 lumbar (two examples middle and bottom-left) and thoracic (top right). The most consistent
775 findings were small ipsilaterally-projecting neurons in the thoracic cord (**C'**), and large neurons
776 contralateral to injury from just lateral to area X to the ventral grey matter in the lumbar cord
777 (**C''**). Arrows in **C'** and **C''** indicate midline-crossing axons. Arrow pointing to tdTomato⁺ axons
778 in dorsal cervical white matter indicates probable rubrospinal (RST) and/or raphespinal tracts.
779 Arrows pointing to reporter-positive axons in ventral white matter indicate probable

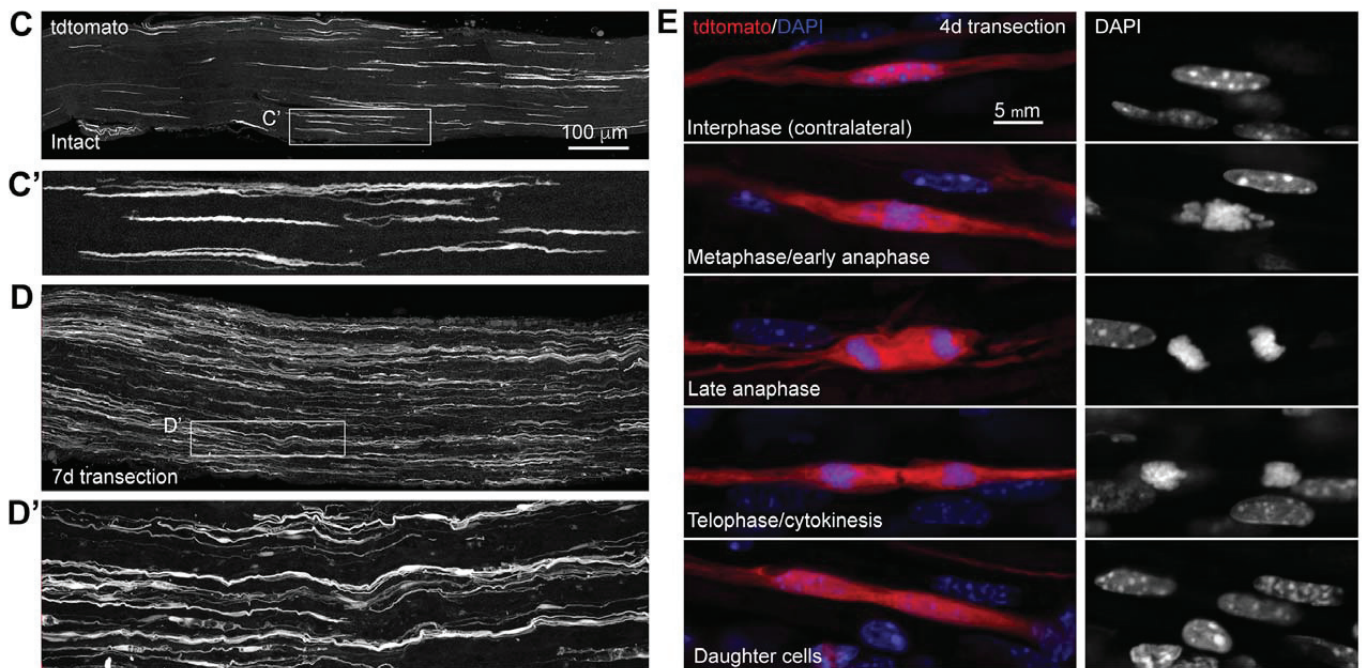
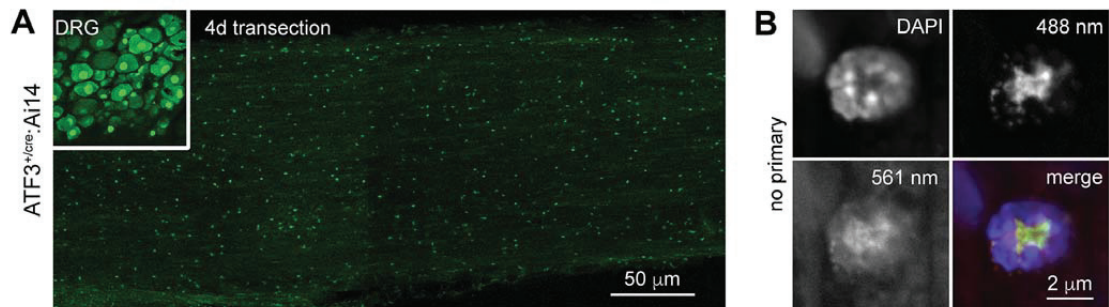
An ATF3^{cre} mouse for axotomy-induced genetic editing.

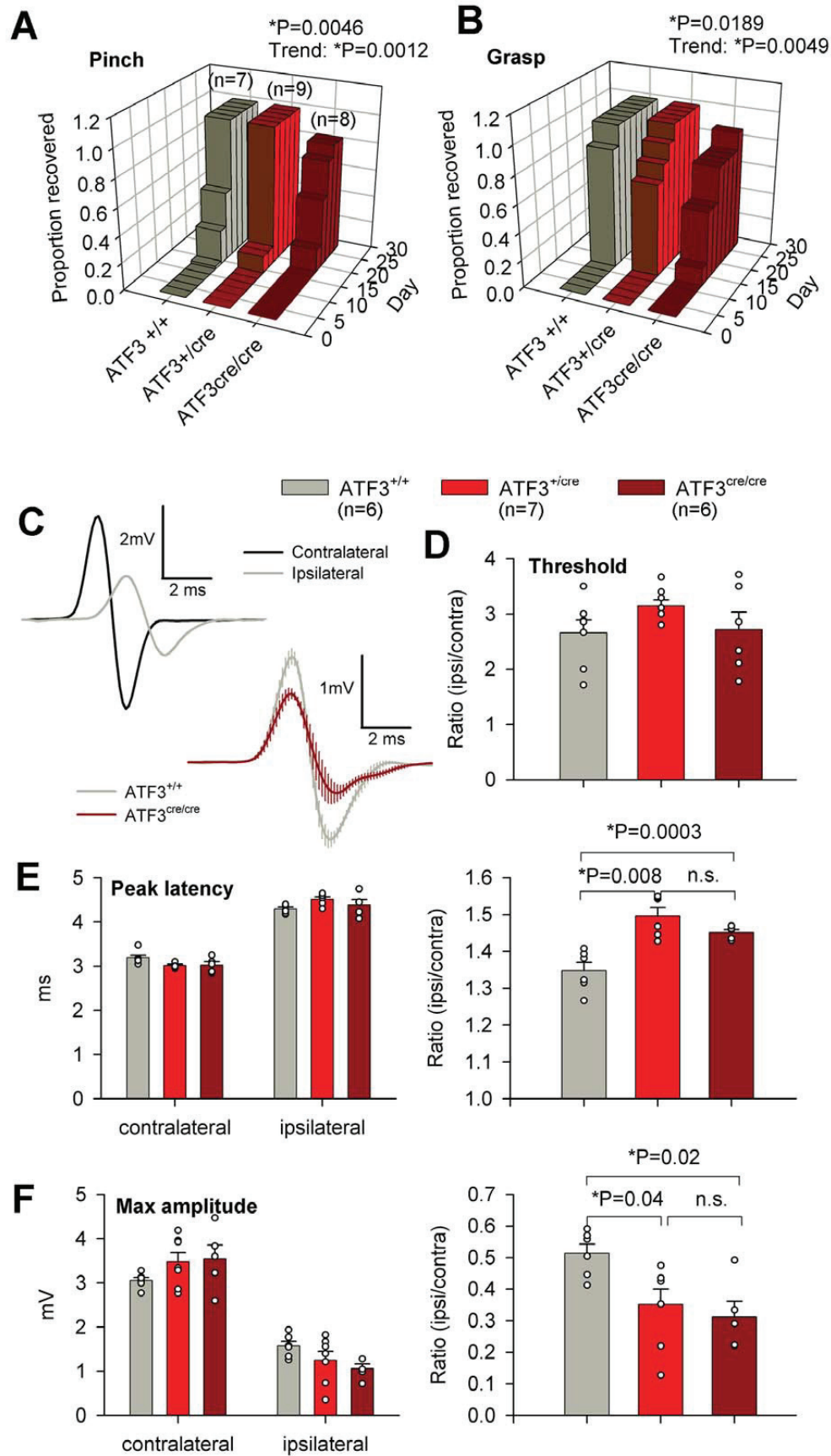
780 reticulospinal (RtST) and vestibulospinal (VST), and an unknown descending projection (?)
781 tracts rostral to the injury, and spinothalamic (STT) and possible dorsal spinocerebellar
782 (DSCT(?)) below the injury (thoracic and lumbar sections). **D**, Neurons in Clarke's column
783 ipsilateral to the hemisection. **E** and **F**, large and small (respectively) putative spinothalamic tract
784 neurons contralateral to the hemisection. Arrows in **E** and **F** indicate commissural axons. cc:
785 central canal.

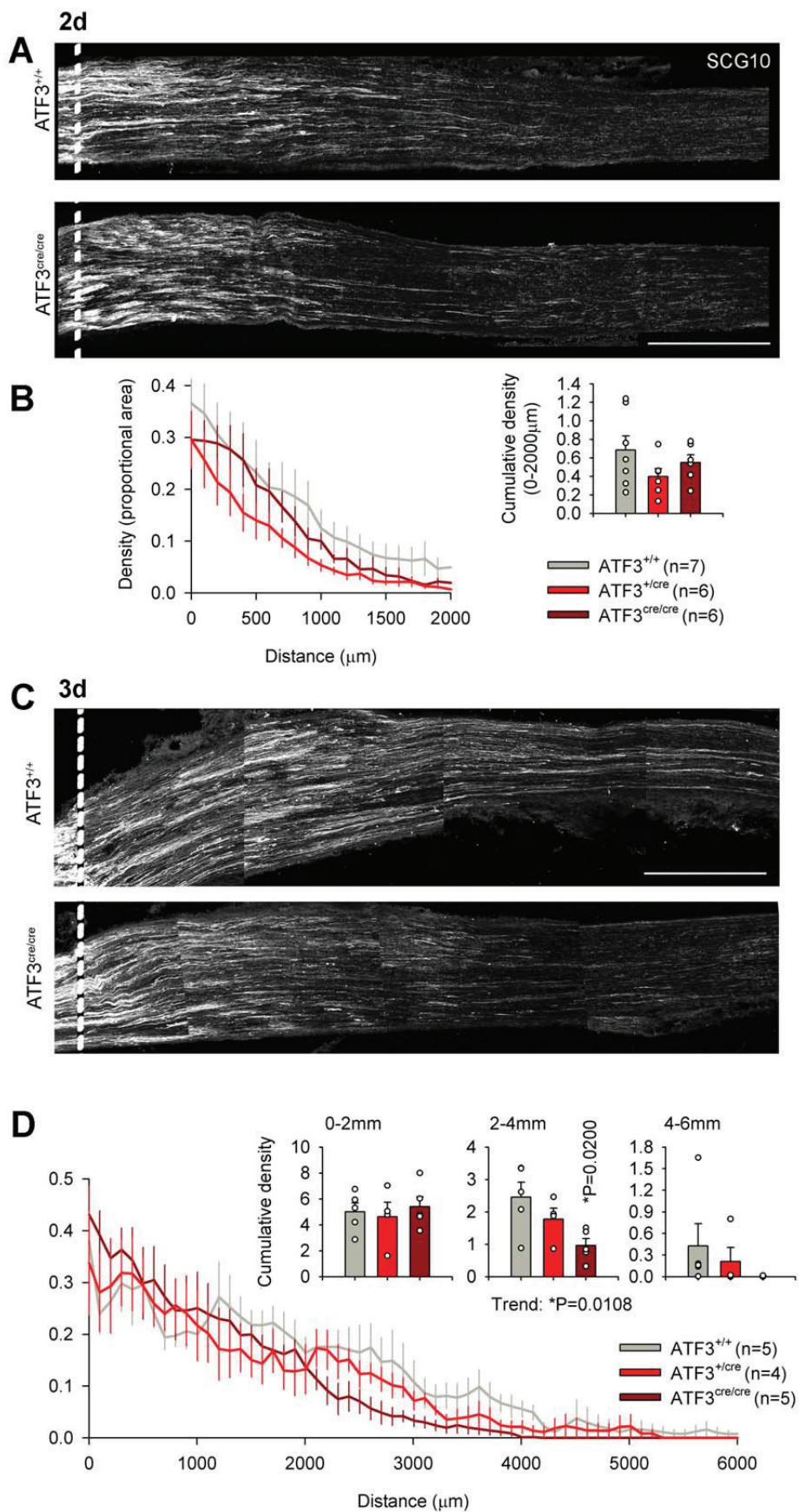
786

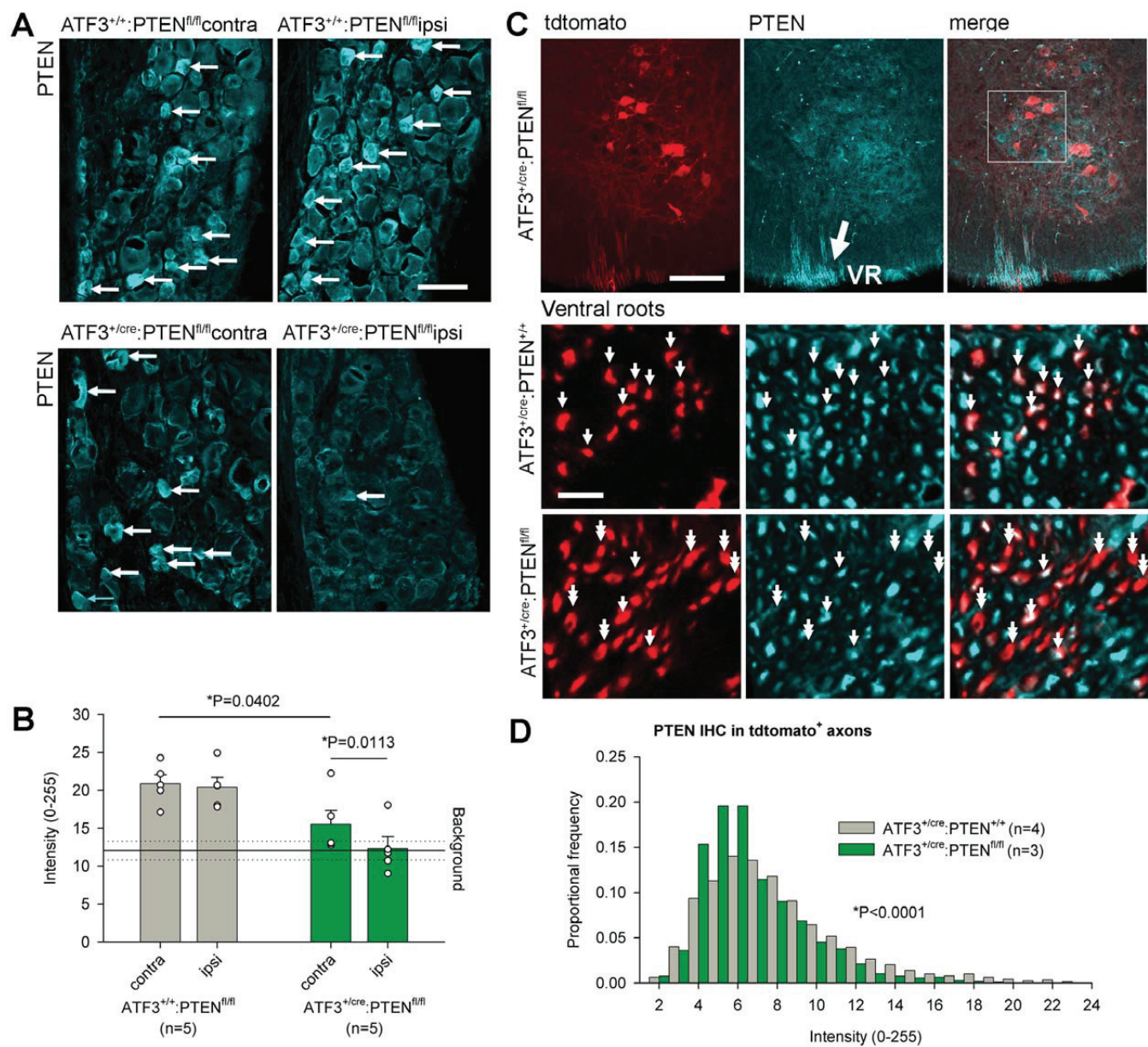
787 **Figure 9. Hemisection-induced recombination in supraspinal neurons one week post-**
788 **injury.** **A**, paraventricular hypothalamic nucleus, descending part. **B**, Red nucleus. **C**,
789 Vestibulospinal nucleus (the genu of the facial nerve is indicated by VII). **D**, reticulospinal
790 neurons (RtS) and raphespinal neurons (arrow), and the rubrospinal tract (RST). **E**, Reporter-
791 expressing axons in the medial longitudinal fasciculus (conveying descending projections of
792 reticulospinal and vestibulospinal axons). **F**, examples of ATF3-positive, tdtomato-positive and -
793 negative neurons in the paraventricular hypothalamic nucleus (PHN), red nucleus (RN),
794 vestibulospinal nucleus (VSN), and reticulospinal neurons (RtS).
795

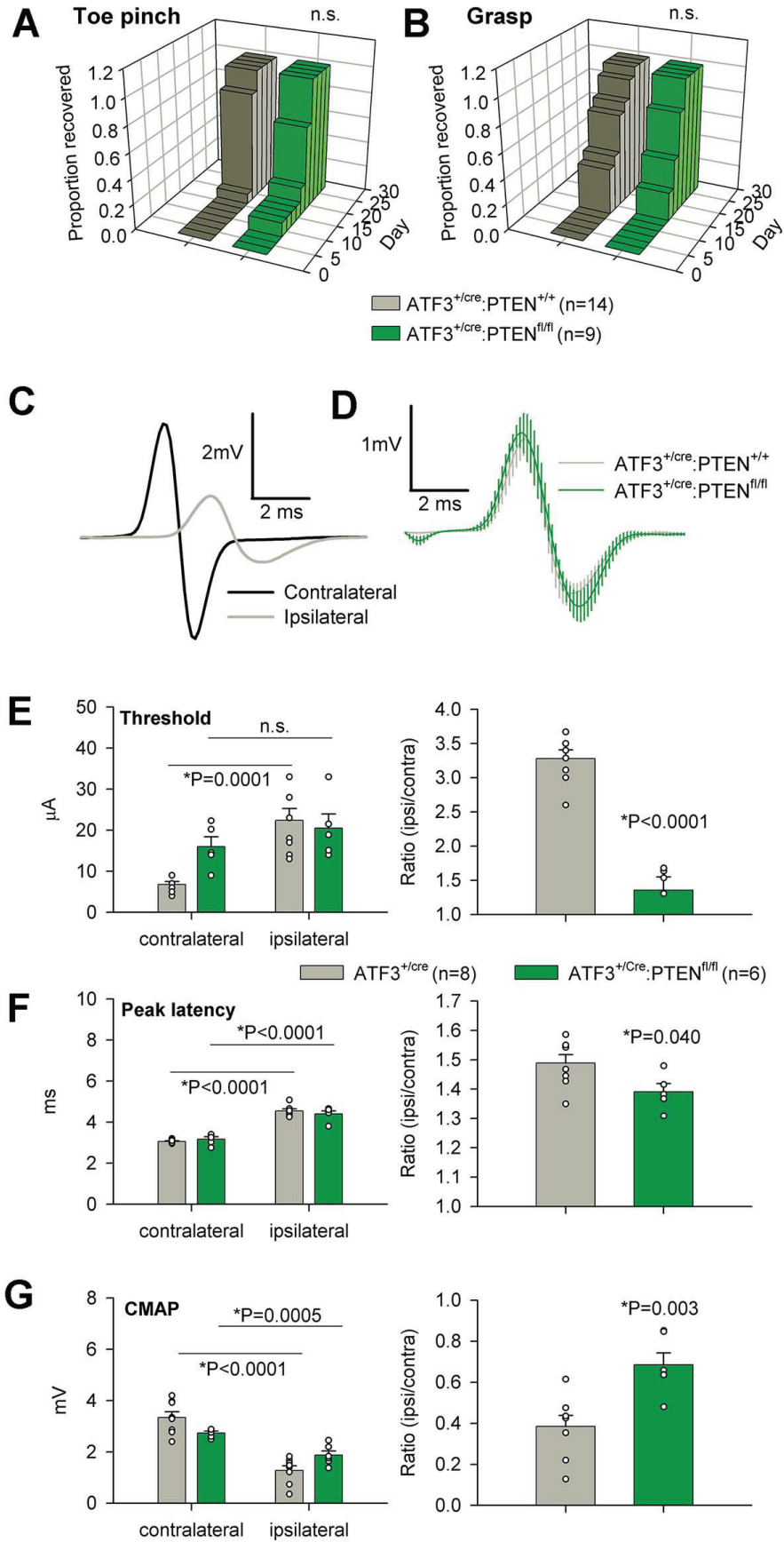


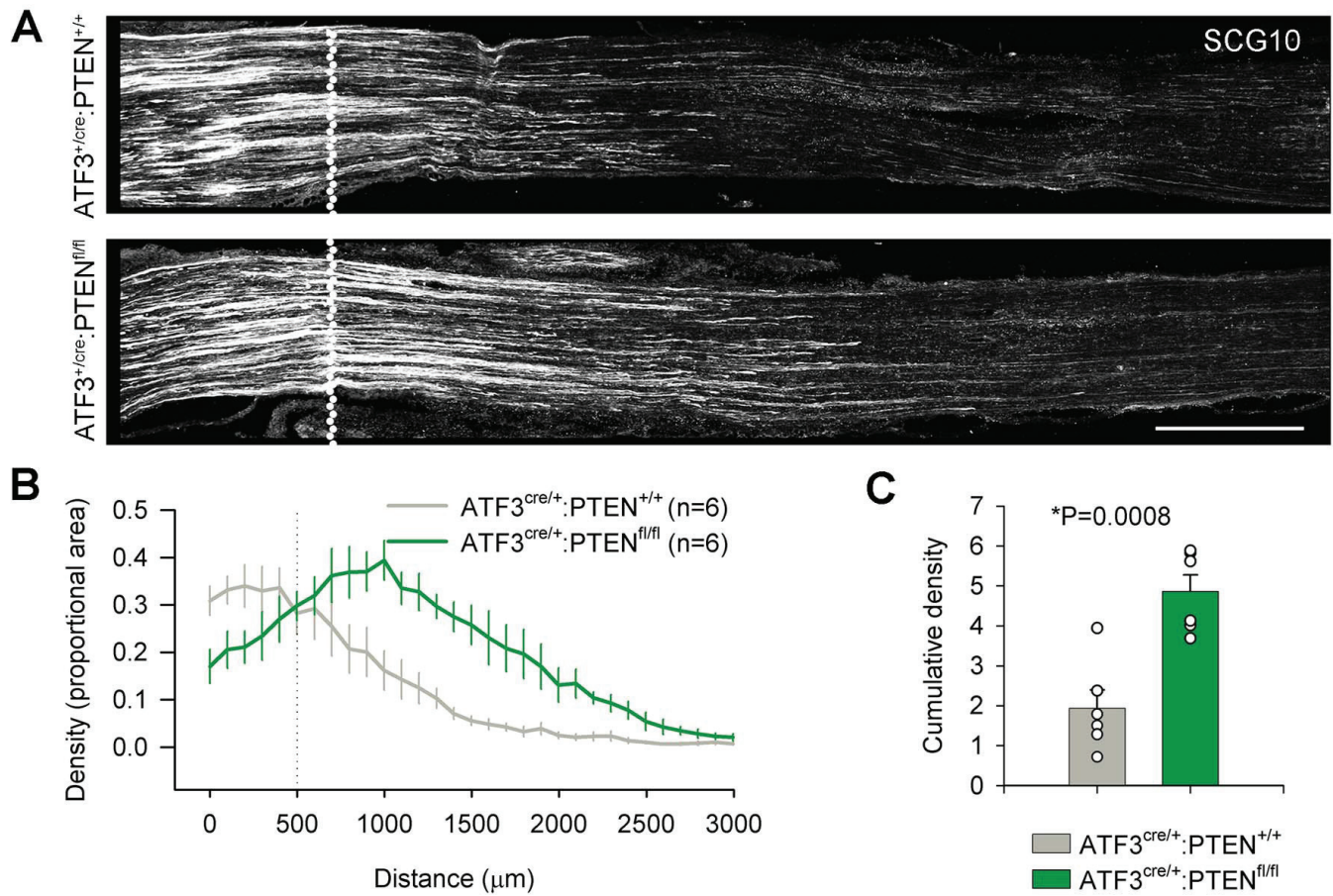












A ATF3^{+cre}:Ai14

